



INVESTIGATIONS ON LIMITATIONS OF THE VIRTUAL ROTATING ARRAY METHOD

Marius Lehmann¹, Carsten Spehr², Marc Schneider¹, Daniel Ernst²

¹ebm-papst Mulfingen GmbH & Co. KG
Bachmühle 2, 74673 Mulfingen, Germany

²German Aerospace Center (DLR)

Abstract

The virtual rotating array method is a widely used approach for the characterization of rotating sound sources. Because of its operation in the frequency domain it has some advantages compared to methods in the time domain. The most important are the extensive applicability of deconvolution algorithms and low computational costs.

In the present study some limitations of the method are shown. A parametric study on several influencing factors is done. The goal is to find out how a ring array must be designed in order for the method to work for a particular test case. It can be shown that the incident sound waves must be spatially sampled with at least two microphones per wavelength for the interpolation to work. This is influenced by the angle of incidence of the sound, which depends on the radius of the source rotation and the ring array as well as their distance.

1 INTRODUCTION

Beamforming with microphone array data has become a standard tool in product design. For the development of fans, rotating beamforming has to be applied. There are various approaches to this: In [9], Sijtsma et al. presented a method in which beamforming is performed in the time domain on a co-rotating focus grid. The time delays and Doppler shifts are recalculated for each time step.

In another group of methods, the microphone array is transformed virtually into a co-rotating reference frame. This is done either by linear interpolation between the stationary microphones (see Dougherty et al. [1] and Herold & Sarradj [3]) or by modal decomposition of the rotating sound field (see Ocker & Pannert [5] and Pannert & Maier [6]).

In [2, 4], Herold et al. and Ocker et al. compared the methods and made an estimate of how many microphones are needed per ring array. However, only one test case is considered for this estimation.

In the present work is deduced which parameters influence the required number of microphones and how they have to be chosen to ensure correct interpolation. For this purpose, different test cases of synthetically generated microphone array data of monopole sound sources are evaluated. The performance of rotating beamforming is compared to that of stationary beamforming. The virtual rotating array [3] is used as interpolation method. Coherence between the array microphones is used as a criterion for the stability of the method. To find the reason for coherence loss, signals of single microphones are investigated and the spatial resolution of the incident sound waves through the individual microphone pairs of the array is calculated.

2 METHODS

In the following, the examined test cases will be given first. Then the mathematical background of beamforming in the frequency domain and the virtual rotating array are described. Finally, the analysis methods used in this paper are introduced.

2.1 Setup

In this study, the performance of the virtual rotating array method for different ring array - source combinations is investigated. The microphone array data is generated synthetically using the acoular [7] class “SamplesGenerator”. Microphone signals are generated for different combinations of source and array parameters. There are both rotating and stationary monopole sources simulated. The source signal is either white noise or a sinusoidal signal at a certain frequency.

The setup is shown schematically in fig. 1. The distance between source and array plane is $z_r = 0.8$ m. The time signals for different source configurations are simulated for an array with radius $r_r = 0.8$ m and $M = 50$ microphones. The x-axis points upwards, the y-axis points to the right and the z-axis points into the plane. The microphones are numbered counterclockwise.

The source positions that are primarily investigated in this paper have trajectories with the radii $r_s = 0.2$ m and $r_s = 0.4$ m. In the rotating cases they move counterclockwise. Figure 1 shows the source position for the larger trajectory $r_s = 0.4$ m.

2.2 Frequency domain beamforming

In the following, a short overview about frequency domain beamforming is given based on [8]. A commonly used approach for beamforming with microphone arrays is based on the auto- and cross- powers of the microphone signals. They are stored in the cross- spectral matrix (CSM):

$$\mathbf{C} = \frac{1}{2} \mathbf{p} \mathbf{p}^* \quad (1)$$

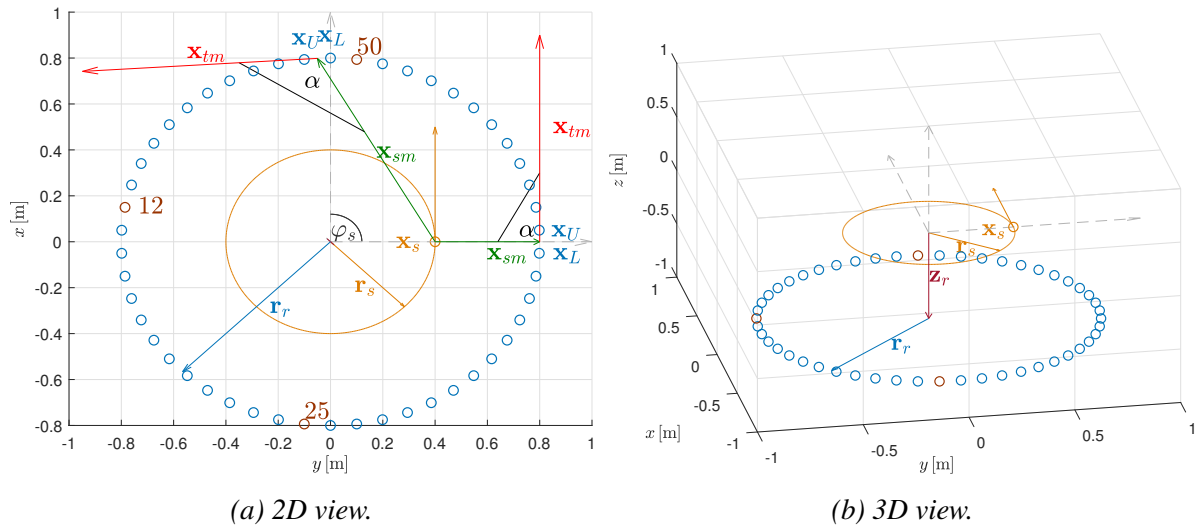


Figure 1: Setup for $M = 50$, $z_r = 0.8\text{m}$ and $r_r = 0.8\text{m}$ and geometric relationships between array and source positions.

For an array of M microphones, \mathbf{p} is the M - dimensional vector of the frequency f dependent complex microphone pressure amplitudes:

$$\mathbf{p} = \begin{pmatrix} p_1(f) \\ \vdots \\ p_M(f) \end{pmatrix} \quad (2)$$

To estimate the source auto-power for a certain focus point, the steering vector \mathbf{g} describing the sound propagation between the focus point and the microphone positions has to be calculated. For the simplest approach, a monopole source under freefield radiation conditions, its components g_m can be calculated as follows:

$$g_m(f) = \frac{1}{r} e^{-jkr_m} \quad (3)$$

The CSM has to be multiplied with the weighted steering vector \mathbf{w} :

$$A = \mathbf{w}^* \bar{\mathbf{C}} \mathbf{w} \quad (4)$$

with the weight vector \mathbf{w} :

$$\mathbf{w} = \mathbf{g} / \left(\sum_{(m,n)} |g_m|^2 |g_n|^2 \right)^{1/2}. \quad (5)$$

(m, n) are all possible combinations of microphones.

2.3 Virtual rotating array

A method to compensate for the motion of rotating sound sources was published by Herold & Sarradj [3]: The array microphones are virtually set into motion synchronous to the sound source. This is done by interpolating the signals of the adjacent, stationary microphones sample by sample at the actual position of the virtual rotating microphones.

The most obvious way for applying this method is to use circular arrays. The angle β between two microphones m depends on the number of microphones per ring M :

$$\beta = \frac{2\pi}{M} \quad (6)$$

The signal $p_{vr,m}$ of a virtual rotating microphone at a certain time step t is calculated by linear interpolation between the adjacent lower and upper microphones m_l and m_u :

$$p_{vr,m}(t) = s_l p_{m_l} + s_u p_{m_u} \quad (7)$$

with the weight factors s_l and s_u depending on the actual source position $\varphi(t)$:

$$\begin{aligned} s_u(t) &= \frac{\varphi(t)}{\beta} - \left\lfloor \frac{\varphi(t)}{\beta} \right\rfloor \\ s_l(t) &= 1 - s_u(t) \end{aligned} \quad (8)$$

$\lfloor \cdot \rfloor$ denotes the floor function.

The virtual microphones are in the same reference frame as the rotating sound sources. Therefore, the CSM can be calculated equivalently to the stationary case (see section 2.2). For the application of beamforming it has to be considered that the medium between source and array plane is not transformed into the rotating reference frame. This has to be taken into account when calculating the retarded times for steering vectors. After calculating the correct retarded times iteratively, frequency domain beamforming based on CSM data can be done and deconvolution algorithms can be applied.

2.4 Coherence between array microphones

Coherence is a measure for the similarity of two signals. In this contribution, it is used to assess the quality of the array microphones transformation from stationary to rotating reference frame. The coherence is calculated as the magnitude squared averaged cross power spectrum of two microphone signals:

$$\gamma_{m,n}^2(f) = \frac{|\langle C_{m,n}(f) \rangle|^2}{\langle C_{m,m}(f) \rangle \cdot \langle C_{n,n}(f) \rangle} \quad (9)$$

A value of one means that the microphone signals are completely linear dependent. For free field propagation this should be the case because the microphone signals are only time shifted and attenuated in dependence of the distances between source and microphone positions. A loss of coherence indicates that the interpolation of the stationary microphone signals failed.

2.5 Spatial sampling of interpolation

The spatial sampling rate of the sound field by the microphone array is used as one criterion for investigating the limitations of the method. For this purpose, the effective wavelength of the sound as a function of the angle of incidence is calculated from the point of view of each adjacent microphone pair.

This is shown schematically in fig. 1a. The angle of incidence α is determined in the middle of each pair of microphones. This location \mathbf{x}_m is calculated from the coordinates of the lower and upper microphone \mathbf{x}_l and \mathbf{x}_u :

$$\mathbf{x}_m = \mathbf{x}_l + \frac{\mathbf{x}_u - \mathbf{x}_l}{2} \quad (10)$$

The sound propagates through the microphone pair along the connection vector $\mathbf{x}_{sm} = \mathbf{x}_m - \mathbf{x}_s$ between the source position \mathbf{x}_s and their center \mathbf{x}_m . The angle of incidence α is calculated between this vector and the tangential vector \mathbf{x}_{tm} at the microphone pair center \mathbf{x}_m using the law of cosines:

$$\alpha = \arccos \left(\frac{\mathbf{x}_{sm} \cdot \mathbf{x}_{tm}}{|\mathbf{x}_{sm}| |\mathbf{x}_{tm}|} \right) \quad (11)$$

The effective wavelength is calculated from the wavelength of the sound $\lambda = \frac{c}{f}$ and the angle of incidence:

$$\lambda_{eff} = \frac{\lambda}{|\cos(\alpha)|} \quad (12)$$

The spatial sampling rate in mics per wavelength (mpw) is the quotient of effective wavelength λ_{eff} and the distance between the microphones $\Delta \mathbf{x}_{lu} = |\mathbf{x}_u - \mathbf{x}_l|$:

$$mpw = \frac{\lambda_{eff}}{\Delta \mathbf{x}_{lu}} \quad (13)$$

3 RESULTS

In this section, the results of the synthetically generated test cases will be discussed. For this purpose, beamforming maps and coherence between individual microphones are first compared for each case. Then, individual microphone signals are evaluated.

3.1 Beamforming maps

In the following, beamforming maps for different source - microphone array combinations are shown. In fig. 2, maps for source trajectory radius $r_s = 0.2$ m are compared to those for $r_s = 0.4$ m. The results are plotted for a single frequency line $f \approx 8$ kHz. The reference array with radius $r_r = 0.8$ m and $M = 50$ microphones was used.

On the left hand side, results for stationary beamforming are shown. This means that microphone signals for a static source at $[x = 0; y = r_s]$ were simulated and stationary beamforming as described in section 2.2 was done.

For the maps on the right hand side, a source rotating at r_s with rotational speed of $n = 1200$ rpm was simulated. The evaluation was done with the VRA- method as described in section 2.3.

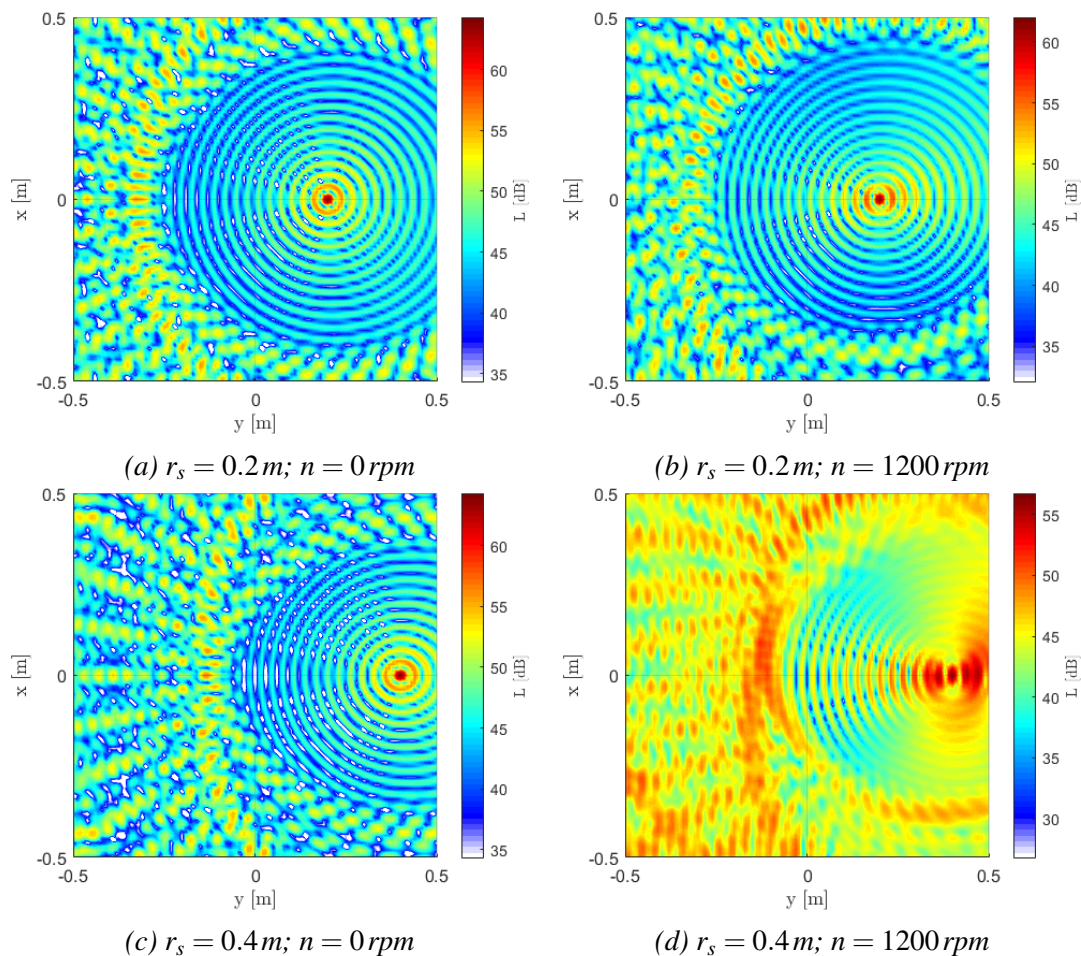


Figure 2: Beamforming maps at $f = 8kHz$ for a synthetic monopole source emitting white noise. Ringarray with $M = 50$ microphones and $r_r = 0.8m$ radius. Distance to source plane $z_r = 0.8m$.

For $r_s = 0.2m$, there are only small differences between the beamforming maps of the stationary and the rotating case. Resolution and dynamic are comparable. The only differences are a slightly lower source level and stronger side lobes in radial direction for the rotating case.

This is not the case for the larger trajectory radius of $r_s = 0.4m$: While the map for the stationary case is still comparable to the previous ones, the following differences exist for the rotating case: The level of the source point is significantly lower, which reduces the dynamic range. Furthermore, there are side lobes of same level as the source in radial direction below and above the source position.

3.2 Array coherence

Looking for reasons for the differences between the beamforming maps, the coherence between the array microphones is calculated according to section 2.4. The results are shown in fig. 3:

For the stationary cases, coherence between all mics is $\gamma^2 \approx 1$. This is not true for the

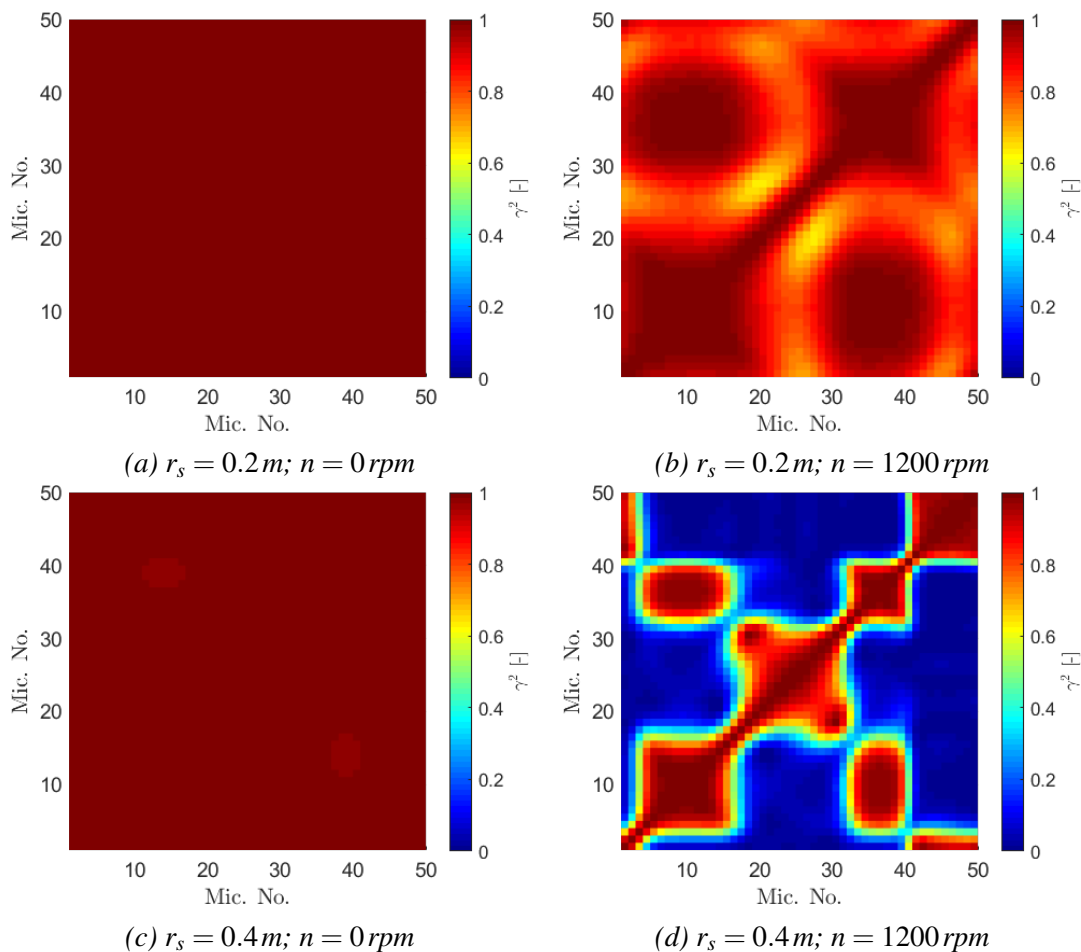


Figure 3: Coherence γ^2 between virtual rotating microphones at $f = 8kHz$ for a synthetic monopole source emitting white noise. Ringarray with $M = 50$ microphones and $r_r = 0.8m$ radius. Distance to source plane $z_r = 0.8m$.

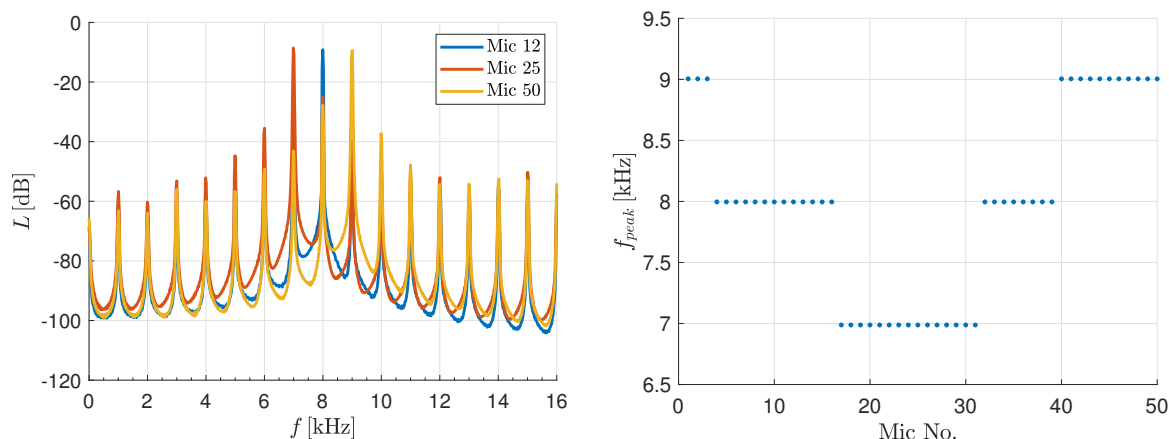
microphone signals from rotating beamforming. There is a loss of coherence between several microphones. For $r_s = 0.2m$, the lowest value of coherence is $\gamma^2 \approx 0.6$. However, there are also spots where coherence remains almost one.

For $r_s = 0.4m$, the spots of high coherence remain at the same position, but they are smaller. For the remaining microphone pairs, however, the coherence drops to values below $\gamma^2 = 0.2$.

3.3 Frequency shift in dependence of microphone position

In fig. 4a, the spectra of three different virtually rotating microphones for a sinusoidal source signal of $f_s = 8kHz$ are compared. The positions of these microphones relative to the source position is shown in fig. 1a. Again, the array radius is $r_r = 0.8m$ and the number of microphones is $M = 50$. The distance between source and array plane is $z_r = 0.8m$.

The first spectrum to be discussed is that of microphone 12. This microphone moves approximately parallel to the source. The spectrum shows the highest peak at the source frequency of $f_s = 8kHz$. In addition, however, further peaks of lower levels at lower and higher frequencies



(a) Spectra of single rotating microphones at different angular positions. (b) Frequency of peak with maximum level over microphone index.

Figure 4: Spectral analysis of single rotating microphones for a sinusoidal source. $f_s = 8 \text{ kHz}$, $r_s = 0.4 \text{ m}$.

can also be found. Their distance to the source frequency is a multiple of $\Delta f = 1 \text{ kHz}$, which is the product of the number of microphones and the rotational speed $\Delta f = M \cdot n = 50 \cdot 20 \text{ Hz} = 1 \text{ kHz}$.

Microphone 25 is located behind the source. In its spectrum the peaks are at the same frequencies, but the highest peak occurs at $f = 7 \text{ kHz}$. For microphone 50, which is located in front of the source, it is the other way round: Here $f = 9 \text{ kHz}$ is the frequency of the highest peak.

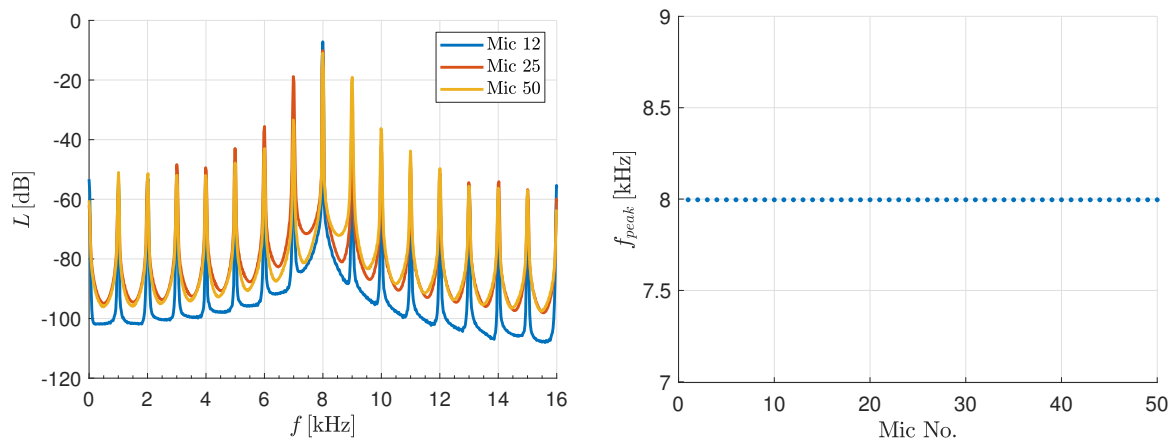
Figure 4b shows the frequency of the highest peak for all microphones in the array. They can be divided into three groups: In the first group (microphone 40-50), the highest peak occurs at a higher frequency. In the second group of microphone 4-16 and 32-39, the peak frequency corresponds to the source frequency. The peak in the microphone spectra of the third group (microphone 17-31) is at too low frequency.

These groups correspond to the three possible forms of relative motion between the rotating source and the stationary microphones, which are the query points for the interpolation of the rotating microphone signals: The rotating microphones of the first group are interpolated from stationary microphones towards which the source is moving. The opposite is true for the third group. In the second group, the relative velocity between source and microphones is small because the source moves parallel to the microphones.

The three areas on the ring array are twisted in relation to the source position. The reason for this is the propagation time between source and array: The signals between which interpolation is taking place were output from the source at a different angle of rotation.

The three microphone groups match the results of the coherence studies with white noise (fig. 3): In the case of the source rotating on the larger radius (fig. 3d), only the microphones in a group are coherent with each other.

In fig. 5 the results for the smaller source trajectory $r_s = 0.2 \text{ m}$ are shown. The frequencies of the different peaks are the same as for $r_s = 0.4 \text{ m}$, but the highest peak is at the frequency of the source $f = 8 \text{ kHz}$ for each microphone. This result also fits in with the findings of



(a) Spectra of single rotating microphones at different angular positions. (b) Frequency of peak with maximum level over microphone index.

Figure 5: Spectral analysis of single rotating microphones for a sinusoidal source. $f_s = 8 \text{ kHz}$, $r_s = 0.2 \text{ m}$.

the coherence studies (fig. 3b): In this case, the coherence between several microphones is significantly smaller than one, but does not approach zero.

4 SPATIAL SAMPLING

In the following section the spatial sampling rate of the sound field by the stationary microphones will be investigated. On the one hand, it will be analyzed how the spatial sampling rate depends on different influencing variables. On the other hand, a rule for the design of a ring array depending on the relevant influencing variables shall be derived.

4.1 Number of microphones per effective wavelength

For the calculation of the spatial sampling rate, the angle of incidence of the sound waves on the different microphone pairs is calculated in order to determine the resulting effective wavelength. The calculations are carried out according to section 2.5. For the geometric relationships see fig. 1a. The results are plotted for the time when the source is at $\varphi_s = 90^\circ$ in the stationary reference frame. For the rotating reference frame this means that a virtually rotating microphone is always interpolated from the signals of the corresponding stationary microphone pair to which the sound is incident at the corresponding angle.

The results for $r_s = 0.2 \text{ m}$ and $r_s = 0.4 \text{ m}$ are shown in fig. 6. In fig. 6a, the incidence angle α of the sound waves for each microphone is plotted over their angular position φ . In fig. 6b, the resulting number of mics per wavelength (mpw) is plotted.

If φ and φ_s are equal or differ by 180° ($\varphi = 90^\circ$ or $\varphi = 270^\circ$), the sound hits the corresponding microphone pair vertically. As a result, the effective wavelength becomes infinitely large and thus the spatial resolution infinitely fine. In between, the angle of incidence differs from $\alpha = 90^\circ$, making the effective wavelength smaller and thus reducing the number of points per wavelength.

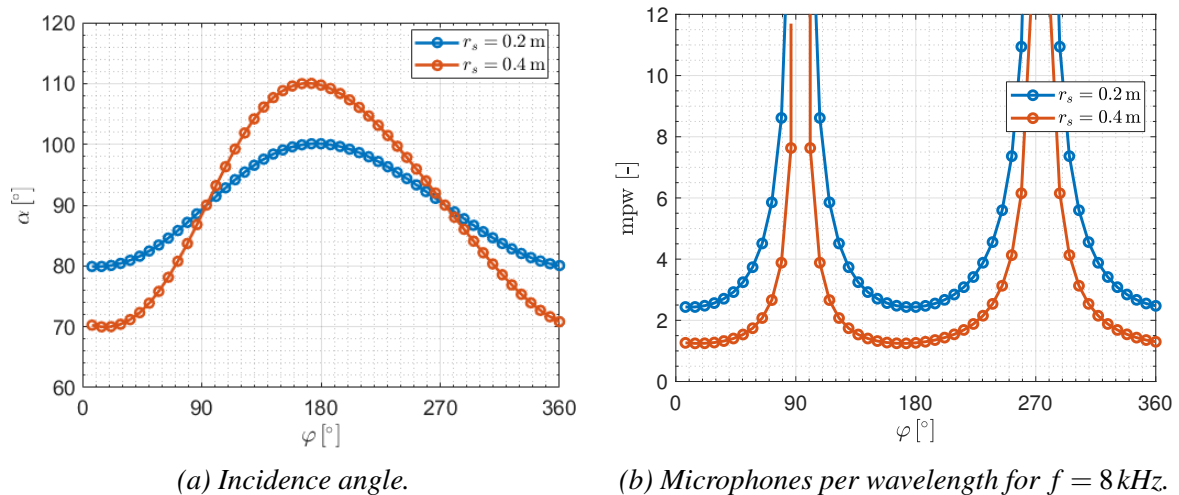


Figure 6: Sound incidence angle α and spatial sampling rate mpw as a function of the angle of rotation φ . $r_r = 0.8$ m, $z_r = 0.8$ m, $M = 50$. Source at $\varphi = 90^\circ$.

The deviation of the angle of incidence doubles when the radius of the source trajectory doubles. This results in approximately twice as fine spatial scanning for the case with small radius.

In case of the larger trajectory radius, the spatial resolution for 28 of 50 microphones is $mpw < 2$. This is almost the same as the number of microphones (29) for which the highest peak in the spectrum does not correspond to the source frequency (Group 1+3 in fig. 4b). The lowest value is $mpw \approx 1.2$.

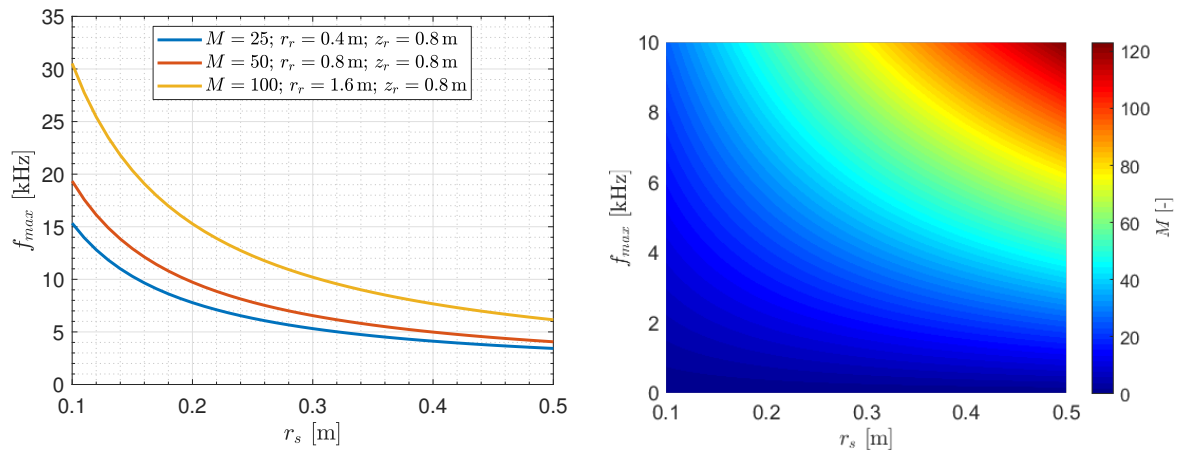
For $r_s = 0.2$ m the lowest resolution is $mpw \approx 2.4$.

4.2 Determination of the maximum evaluable frequency

In the following, the dependence of the spatial resolution on the individual parameters will be derived. According to eq. 13, the lowest spatial resolution is achieved when the effective wavelength is small. This is the case when the magnitude of the cosine of the angle of incidence $|\cos(\alpha)|$ becomes large (see eq. 12). Therefore, analogous to eq. 11, the dependence of $|\cos(\alpha)|$ on the angle of rotation φ is to be determined by means of the cosine theorem.

The analysis takes place in the rotating reference system. This means that the source is at a certain angle of rotation φ_s . For $\varphi_s = 90^\circ$ and a trajectory radius r_s the source coordinates are $\mathbf{x}_s = (0 \ r_s \ 0)$. The microphone positions on the array ring are defined by $\mathbf{x}_m = (r_r \cos(\varphi_m) \ r_r \sin(\varphi_m) \ z_r)$. This results in the connection vector between source and microphone positions:

$$\mathbf{x}_{sm} = \begin{pmatrix} r_r \cos(\varphi_m) \\ r_r \sin(\varphi_m) - r_s \\ z_r \end{pmatrix} \quad (14)$$



(a) Maximum evaluable frequency in dependence of radius of source trajectory. (b) Minimum required number of microphones for $r_r = 0.8$ m and $z_r = 0.8$ m.

Figure 7: Maximum evaluable frequency ensuring that $mpw > 2$ is fulfilled for each microphone pair.

The tangential vector in interpolation direction is defined as follows:

$$\mathbf{x}_{lm} = \begin{pmatrix} \sin(\varphi_m) \\ -\cos(\varphi_m) \\ 0 \end{pmatrix} \quad (15)$$

with $|\mathbf{x}_{lm}| = 1$. According to eq. 11 the cosine of the angle of incidence of sound is obtained:

$$\cos(\alpha) = -\frac{r_s \cos(\varphi_m)}{\sqrt{r_r^2 - 2r_r r_s \sin(\varphi) + r_s^2 + z_r^2}} \quad (16)$$

To determine the extreme values of the function, the roots of the derivative according to φ must be calculated:

$$\frac{d \cos \alpha}{d \varphi} = \frac{r_s \sin(\varphi)}{\sqrt{r_r^2 - 2r_r r_s \sin(\varphi) + r_s^2 + z_r^2}} - \frac{r_r r_s^2 \cos^2(\varphi)}{(r_r^2 - 2r_r r_s \sin(\varphi) + r_s^2 + z_r^2)^{\frac{3}{2}}} = 0 \quad (17)$$

Equation 17 cannot be solved explicitly. For concrete test cases, however, the maximum of eq. 16 can be calculated and, based on this, the influencing variables can be determined in such a way that $mpw > 2$ is always fulfilled.

Figure 7a shows the maximum evaluable frequency as a function of the radius of the source trajectory for three different ring arrays. The orange line shows the course for the ring of the previous tests. For the smaller trajectory radius $r_s = 0.2$ m the maximum frequency $f_{max} \approx 9.7$ kHz is larger than the investigated frequency $f = 8$ kHz. For the larger rotation radius $r = 0.4$ m the maximum frequency is $f_{max} \approx 5$ kHz and is thus significantly smaller than the investigated frequency.

For comparison, the curves for microphone rings half the size and twice the size are plotted at

the same axial position. The number of microphones has also been halved or doubled in order to achieve a constant microphone distance. The maximum frequency increases with increasing ring radius. This means that the number of microphones must be increased but not doubled if the ring diameter is to be doubled and the maximum frequency is to remain the same. With larger ring diameter, the microphone distance also can be increased.

To design a microphone array for a rotating sound source localization, a diagram as in fig. 7b can be used: First, the array must be designed for the stationary case. The ring diameter r_r and the axial distance z_r must be set in such a way that a suitable point spread function is obtained. Several microphone rings can also be used for this purpose. Then a diagram analogous to fig. 7b must be generated for each ring. From this diagram, the radius of the rotating test object and the maximum frequency to be examined can be used to determine the number of required microphones for each ring.

5 CONCLUSIONS

In the present study the limitations of the virtual rotating array method were investigated. Therefore the beamforming maps of different stationary and rotating synthetically generated test cases were compared. A monopole emitting white noise was used as a source.

It was shown that the results of the rotating cases differ from those of the stationary cases above a certain rotation radius of the sources for a fixed frequency. This trend can also be observed when comparing the coherence between the array microphones for the individual setups: Above a certain rotation radius, the coherence between some pairs of microphones approaches zero, but for others it remains close to one.

In the next step, the signals of individual microphones were examined. Instead of white noise, a sine wave at the corresponding frequency was used as the source signal. In the spectra, in addition to a peak at the frequency of the sine, other peaks appear. Their distance from the source frequency depends on the number of microphones and the speed of rotation. Starting at a certain source rotation radius, the peak with the highest amplitude for certain microphone groups shifts to one of these side frequencies. The individual microphone groups correspond to blocks of high coherence in the coherence matrix.

Next, the spatial resolution of the incident sound waves through the individual microphone pairs of the array was investigated. The effective wavelength and the spatial sampling rate were calculated as a function of the angle between the direction of sound propagation and the direction of interpolation. It was shown that in those areas where interpolation fails, the sampling rate is below two microphones per wavelength.

Therefore, in the last step a rule was derived with which the number of microphones can be calculated for a concrete application so that the spatial sampling rate is sufficient.

REFERENCES

- [1] R. Dougherty, B. Walker, and D. Sutliff. "Locating and quantifying broadband fan sources using in-duct microphones." In *16th AIAA/CEAS aeroacoustics conference*, page 3736. 2010. URL <https://ntrs.nasa.gov/archive/nasa/casi.ntrs.nasa.gov/20110003094.pdf>.

- [2] G. Herold, C. Ocker, E. Sarradj, and W. Pannert. “A comparison of microphone array methods for the characterization of rotating sound sources.” In *Proceedings of the 7th Berlin Beamforming Conference*, pages 1–12. 2018. URL <https://pdfs.semanticscholar.org/99e2/9ec8372c9bb0d85a15d3b587d7df161bac73.pdf>.
- [3] G. Herold and E. Sarradj. “Microphone array method for the characterization of rotating sound sources in axial fans.” *Noise Control Engineering Journal*, 63(6), 546–551, 2015. doi:10.3397/1/376348. URL <https://pdfs.semanticscholar.org/430b/2181676a17d73462643eab5fbbce49e33e99.pdf>.
- [4] C. Ocker, G. Herold, F. Krömer, W. Pannert, E. Sarradj, and S. Becker. “Comparison of microphone array methods for the characterization of rotating broadband noise sources.” In *Fan 2018 - International Conference of Fan Noise*. 2018.
- [5] C. Ocker and W. Pannert. “Imaging of broadband noise from rotating sources in uniform axial flow.” *AIAA Journal*, pages 1185–1193, 2017. doi:10.2514/6.2016-2899. URL https://www.researchgate.net/profile/Christof_Ocker/publication/303601749_Imaging_of_Broadband_Noise_from_Rotating_Sources_in_Uniform_Axial_Flow/links/5ddf7d26a6fdcc2837f06592/Imaging-of-Broadband-Noise-from-Rotating-Sources-in-Uniform-Axial-Flow.pdf.
- [6] W. Pannert and C. Maier. “Rotating beamforming–motion-compensation in the frequency domain and application of high-resolution beamforming algorithms.” *Journal of Sound and Vibration*, 333(7), 1899–1912, 2014. doi:10.1016/j.jsv.2013.11.031.
- [7] E. Sarradj and G. Herold. “A python framework for microphone array data processing.” *Applied Acoustics*, 116, 50–58, 2017. doi:10.1016/j.apacoust.2016.09.015.
- [8] P. Sijtsma. “Experimental techniques for identification and characterisation of noise sources.” 2004. URL <https://reports.nlr.nl/bitstream/handle/10921/577/TP-2004-165.pdf?sequence=1>.
- [9] P. Sijtsma, S. Oerlemans, and H. Holthusen. “Location of rotating sources by phased array measurements.” In *7th AIAA/CEAS Aeroacoustics Conference and Exhibit*, page 2167. 2001. URL <https://reports.nlr.nl/xmlui/bitstream/handle/10921/747/TP-2001-135.pdf?sequence=1&isAllowed=y>.